Journal of Power Technologies 101 (1) (2021) 62–69

A Buck-Boost Controlled Full Bridge LED Driver with Zero-Voltage Switching

Kasi Ramakrishnareddy Ch[1], SettingsK Ranjith Kumar[1], and M Surya Kalavathi[2,✉]

[1]Department of Electrical and Electronics Engineering, Vaagdevi College of Engineering, Warangal, India
[2]Department of Electrical EngineeringJNTU College of Engineering Hyderabad,India
✉munagala12@yahoo.co.in

Abstract

A full bridge driver circuit with modulated input voltage using buck-boost converter for LED lighting systems is proposed. A dc voltage source, which is in series, processes portion of lamp power without conversion. Small controlled power is supplied through full bridge circuit. In the proposed configuration, current stress of switches in full bridge is greatly reduced. In addition, zero-voltage switching (ZVS) is accomplished in full bridge devices. Input voltage variations can be compensated to maintain constant LED lamp current. All LED lamps are dimmed simultaneously using on-off control. The circuit description and analysis are discussed in detail and it is validated experimentally.

Keywords: Buck-boost converter, Zero-voltage switching, Full bridge LED driver

1 Introduction

Energy conservation can be improved with efficient use of electrical energy in lighting applications [1]. Thus, use of light emitting diodes (LEDs) in lighting applications is being increased significantly. This is due to their promising features like high efficacy, long life, compact size, solid state characteristic, good colour rendering property, etc. [2]; [3]; [4]. LEDs require DC voltage. For constant illumination LEDs must be operated by either constant current linear regulators or switched mode power regulators [5]. Switched mode power regulators are typically preferred due to their high efficiency [6].

Several types of driver circuits for LED lighting applications have been proposed by researchers based on the availability of driving sources, such as AC fed LED drivers [7]; [8]; [9]; [10]; [11] and DC fed LED drivers [12]; [13]; [14]; [15]; [16]; [17]; [18]. AC fed LED drivers and DC fed LED drivers have different requirements. That said, high efficiency, LED load current regulation, dimming control, compact size and high reliability are the main requirements any LED driver circuit must meet, irrespective of the driving source. Recently, there has been increased use of soft-switching converters in LED lighting applications due to their high efficiency, compactness and low EMI. There is a family of dimmable dc fed zero-current switching (ZCS) quasi resonant converters [19]. A resonant driver is proposed for powering two different LED lamps with independent dimming and regulation [20]. A variable inductor based half bridge LED driver with zero-voltage switching (ZVS) is introduced in [21]. Both dimming and control of lamp current are achieved by variable inductor. Input controlled CLL based resonant dc-dc converter is used [22] for power multiple LED strings. For driving multiple LED loads, a buck-boost integrated half-bridge (HB) series loaded resonant converter is proposed [23]. In [24], a two output coupled inductor (CI) high step down buck converter with ZVS is proposed. Class-E resonant converter with modification is used as the current regulator for an LED lamp in [25]. A high frequency resonant LED driver is introduced in [26]. This driver features independent load current with high efficiency for wide range. This paper proposes a full bridge driver, which integrates advantages such as a small amount of processed power, reduced switch current stress, soft-switching operation, high efficiency and a dimming and regulation feature. This driver can power multiple LED lamps. This study is organized as follows: Section 2 describes the proposed full bridge driver. Section 3 presents the LED driver working principle and analysis. Section 4 presents the design procedure. Section 3 explains the regulation and dimming feature of LED current. The simulation results and conclusion are provided in sections 6 and 7 respectively.

2 Proposed Full Bridge Driver

The proposed full bridge driver for LED lighting systems is shown in Fig. 1. It consists of four power

MOSFETs S_1, S_2, S_3, and S_4. Each MOSFET is represented with an intrinsic body diode and output capacitance. This driver powers four identical LED lamps. An inductor, in series, is used to reduce ripple in each LED lamp current. An inductor L_s is connected between two legs of full bridge. The current in L_s helps to achieve ZVS in full bridge devices. To utilize v-i characteristics of LED, each LED lamp has a dc voltage source, which is in series. It provides most of the lamp's power directly. Full bridge circuit supplies require controlled power. In the proposed LED driver, a buck-boost converter is used to regulate LED lamp currents. It modulates V_{in} which is the input voltage to the full bridge circuit. Switch S_d turns on and off the full bridge circuit at low frequency for the purpose of dimming the LED lamps.

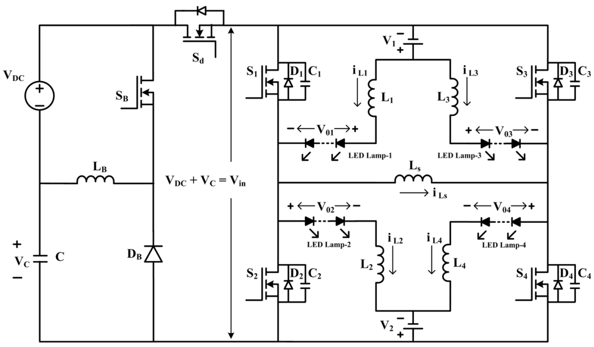

Figure 1: Proposed full bridge LED driver circuit

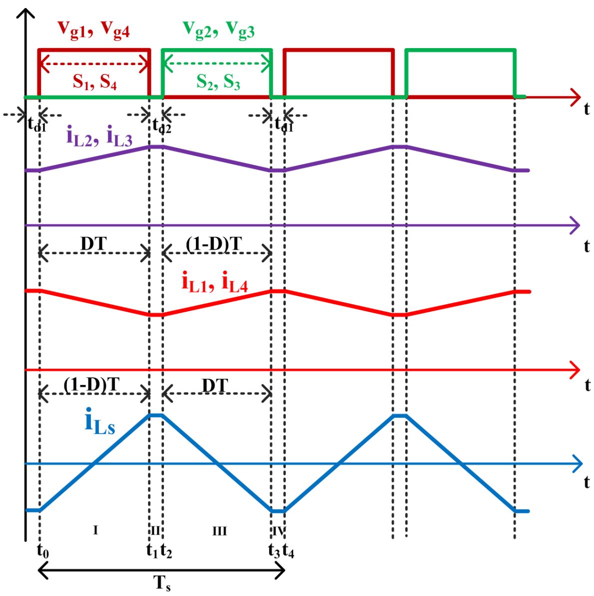

Figure 2: Operating waveforms of proposed LED driver circuit

3 Principle of Operation and Analysis

3.1 Principle of Operation

The operating waveforms are shown in Fig. 2. The switching period is divided into four operating modes and the equivalent circuit in each operating mode is shown in Fig. 3. In this section, the operating modes are explained.

Mode-I (t_0-t_1): At $t = t_0$, gate control voltages are given for switches S_1 and S_4. Inductors L_2 and L_3 charge linearly and inductors L_1 and L_4 discharge linearly. As the voltage across L_s is $+V_{in}$, current through it increases linearly through the devices S_1 and S_4. At the same time, the current (i_{L2} - i_{L1}) flows through S_1 and current (i_{L3} - i_{L4}) flows through S_4. Hence, switch conduction losses mainly depend upon i_{Ls}. This feature reduces switch current stress. This mode ends when inductor current i_{Ls} reaches positive maximum.

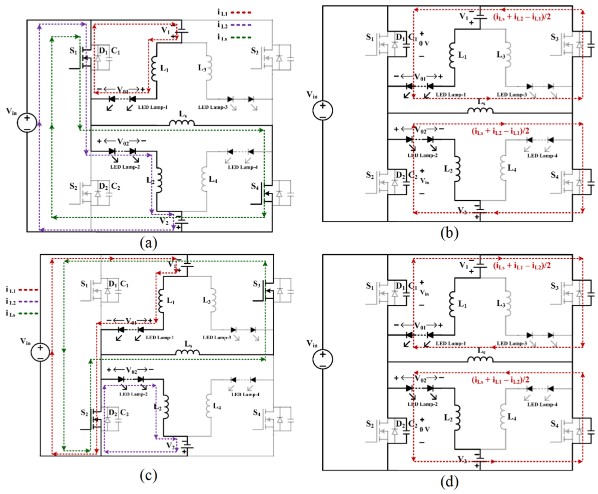

Figure 3: Equivalent circuits of proposed LED driver. (a) Mode-I. (b) Mode-II. (c) Mode-III. (d) Mode-IV.

Mode-II (t_1-t_2): At $t = t_1$, the gate control voltages for devices S_1 and S_4 are removed at zero voltage. During t_1 to t_2, current $(i_{Ls} + i_{L2} - i_{L1})/2$ charges C_1 and discharges C_2. Similarly, capacitor C_4 is charged and capacitor C_3 is discharged $(i_{Ls} + i_{L3} - i_{L4})/2$. After this, switch body diodes D_2 and D_3 are turned on. Now the gate control voltages for S_2 and S_3 may be given for zero voltage turn on. This mode ends at $t = t_2$.

Mode-III (t_2-t_3): Gate control voltages are applied for S_2 and S_3 at $t = t_2$. Inductors L_2 and L_3 discharge linearly and inductors L_1 and L_4 charge linearly. In this mode, current through L_s reduces linearly and it flows through S_2 and S_3. At the same time, the current (i_{L1} - i_{L2}) flows through S_2 and current (i_{L4} - i_{L3}) flows through S_3. Hence S_2 and S_3 carry ripple current in the inductor, which is very small and i_{Ls}. This feature reduces switch conduction losses. This mode ends when current i_{Ls} reaches negative maximum.

Mode IV (t_3-t_4): During t_3 to t_4, switches S_2, $S_3$are switched off and switches S_1, S_4 are switched on at zero voltage. This process is similar to that in mode II. This mode ends at $t = t_4$.

3.2 Analysis

The following assumptions are made to analyze the proposed full bridge LED driver:

- The LED driver is operating in steady state.
- The switches used are ideal.
- Continuous conduction mode.
- Four LED lamps are identical.
- The output voltage across each LED lamp is constant.

In the proposed LED driver, the on and off time of switches S_1 to S_4 is equal and constant. In addition, the switching frequency of S_1 to S_4 is also constant. It is assumed that four LED lamps are identical and their operating currents are the same. Hence the analysis is shown only for LED lamp-1. At $t = t_0$, gate voltages are applied for switches S_1 and S_4. From the equivalent circuit shown in Fig. 3 (a), voltage across inductor L_1 is expressed as

$$\begin{aligned} v_{L1} &= -V_{01} + V_1 \\ &= L_1 \tfrac{di_{L1}}{dt}, t_0 \le t < t_1 \end{aligned} \tag{1}$$

The current through inductor L_1 is obtained as

$$\begin{aligned} &i_{L1}(t) = \tfrac{1}{L_1} \int_{t_0}^{t} v_{L1}(t)\ dt\ + i_{L1}(t_0) \\ &= \tfrac{-V_{01}+V_1}{L_1}(t-t_0) + i_{L1}(t_0) \\ &t_0 \le t < t_1 \end{aligned} \tag{2}$$

Where $i_{L1}(t_0)$ is the initial current in inductor L_1 at time $t = t_0$.

From Eqn. 2, the ripple current in inductor L_1 is calculated as

$$\begin{aligned} &\triangle i_{L1}(t) = i_{L1}(t_1) - i_{L1}(t_0) \\ &= \tfrac{-V_{01}+V_1}{L_1}(t_1 - t_0) \\ &= \tfrac{-V_{01}+V_1}{L_1} DT \end{aligned} \tag{3}$$

Where D is duty ratio of switches S_1 and S_4, and T is the switching period.

Due to positive voltage across L_s, its current increases linearly and is given as

$$\begin{aligned} &i_{Ls} = \tfrac{V_{in}}{L_s}(t-t_0) + i_{Ls}(t_0) \\ &t_0 \le t < t_1 \end{aligned} \tag{4}$$

During t_2 to t_3, switches S_1 and S_4 are in off state. From the equivalent circuit shown in Fig. 3(c), the voltage across inductor L_1 is expressed as

$$\begin{aligned} v_{L1} &= V_{in} + V_1 - V_{01} \\ &= L_1 \tfrac{di_{L1}}{dt} \quad t_2 \le t < t_3 \end{aligned} \tag{5}$$

The current through inductor L_1 is obtained as

$$\begin{aligned} &i_{L1}(t) = \tfrac{1}{L_1} \int_{t_2}^{t} v_{L1}(t)\ dt\ + i_{L1}(t_2)\,e \\ &= \tfrac{V_{in}+V_1-V_{01}}{L_1}(t-t_2) + i_{L1}(t_2) \\ &t_2 \le t < t_3 \end{aligned} \tag{6}$$

Where $i_{L1}(t_2)$ is the initial current in inductor L_1.

From Eqn. (6), the ripple current in inductor $L_1$is calculated as

$$\begin{aligned} &\triangle i_{L1}(t) = i_{L1}(t_3) - i_{L1}(t_2) \\ &= \tfrac{V_{in}+V_1-V_{01}}{L_1}(t_3 - t_2) \\ &= \tfrac{V_{in}+V_1-V_{01}}{L_1}(1-D)T \end{aligned} \tag{7}$$

Where D is duty ratio of switches S_1 and S_4 and T is the switching period.

Due to negative voltage across L_s, its current decreases linearly and is given as

$$\begin{aligned} &i_{Ls}(t) = \tfrac{-V_{in}}{L_s}(t-t_2) + i_{Ls}(t_2) \\ &t_2 \le t < t_3 \end{aligned} \tag{8}$$

By applying volt-sec balance on L_1, the voltage across LED lamp-1 is obtained as

$$[i_{L1}(t_1) - i_{L1}(t_0)] + [i_{L1}(t_3) - i_{L1}(t_2)] = 0 \tag{9}$$

$$\frac{-V_{01}+V_1}{L_1} DT + \frac{V_{in}+V_1-V_{01}}{L_1}(1-DT) = 0 \tag{10}$$

$$V_{01} = DV_{in} + V_1 \tag{11}$$

The above analysis is also applicable for other LED lamps. Hence by using eqns. (3), (7), and (11), the ripple current through each LED lamp and voltage across each LED lamp are given by

$$V_{0k} = DV_{in} + V_j \tag{12}$$

$$\begin{aligned} \triangle i_{Lk} &= \frac{V_{in}+V_j-V_{0k}}{L_k}(1-D)T \\ &= \frac{-V_k+V_j}{L_k}DT \end{aligned} \tag{13}$$

where k = 1, 2, 3, 4 and j = 1, 2

After selecting ripple current, Eqn. (13) can be used to calculate the values of L_1, L_2, L_3, and L_4.

4 Design Considerations

The equivalent parameters of LED lamp are required to calculate the component values in the proposed LED driver. LED can be modelled as series connection of a cut-in or threshold voltage V_{th}, a dynamic resistance r_d and an ideal diode. In the proposed LED driver, 4 LED lamps are used. Each LED lamp is operated at 33 V, 1.1A and has a cut-in voltage of 23.6 V. The power rating of each lamp is 36 W.

The input voltage V_{in} to the full bridge can be expressed from (12) as

$$V_{in} = \frac{V_{0k} - V_j}{D} \tag{14}$$

As the LED lamp does not produce illumination below cut-in voltage, V_j is chosen as 24 V. All switches in full bridge are operated with fixed duty ratio of 0.5. With V_{0k} of 33 V, the input voltage is calculated as

$V_{in} = \frac{33-24}{0.5} = 18V$

From Eqn. (13), the value of inductor L_k is expressed as

$$L_k = \frac{V_{in}+V_j-V_{0j}}{\triangle i_{Lk}}(1-D)T \tag{15}$$

For a switching frequency of 200 kHz and ΔL_k of 10%, the value of L_k can be calculated from (15) as

$$L_k = \frac{18+24-33}{0.11}(0.5)\left(5\cdot 10^{-6}\right)$$

$$\equiv 205\mu H$$

Inductor L_s was used to achieve zero-voltage switching in switches in full bridge during dead time. Since the shape of current in L_s is triangular, only peak current needs to be considered for ZVS. This peak current charges and discharges switch output capacitors during dead time for ZVS. And it is assumed that during dead time peak current through L_s is constant and its value is obtained as

$$i_{Ls-pk} = \frac{V_{in}T}{4L_s} \tag{16}$$

For V_{in} of 18 V, T of 5 µs and L_s value of 33μH, $i_{Ls\text{-}pk}$ is calculated as

$i_{Ls-pk} = \frac{(18)(5)\left(10^{-6}\right)}{(4)(33)\left(10^{-6}\right)} = 0.68A$

5 Regulation of LED Lamp Current and Dimming Control

Dimming control is a key feature in present LED lighting applications. In the proposed LED driver, pulse width modulation (PWM) dimming is provided by using switch S_d, which entirely switched ON and OFF the full bridge. Thus the average illumination level in each LED lamp can be changed without changing the nominal current. To minimize flickering, the operating frequency of switch S_d is selected to be 100 Hz.

The switches in full bridge are operated with fixed duty cycle. Hence LED lamp currents must be regulated against variations in V_{DC}, V_1, and V_2. A buck-boost converter with V_{DC} as input produces controllable voltage V_C at the input side. This controllable voltage V_C compensates the variations in V_{DC}, V_1, and V_2. The gate voltage of switch $S_B$in buck-boost converter must be synchronized with gate voltage of dimming switch S_d to avoid overshoots in V_{in}. Gate voltages of switches S_d and S_B, LED lamp voltage and current under dimming control are shown in Fig. 4.

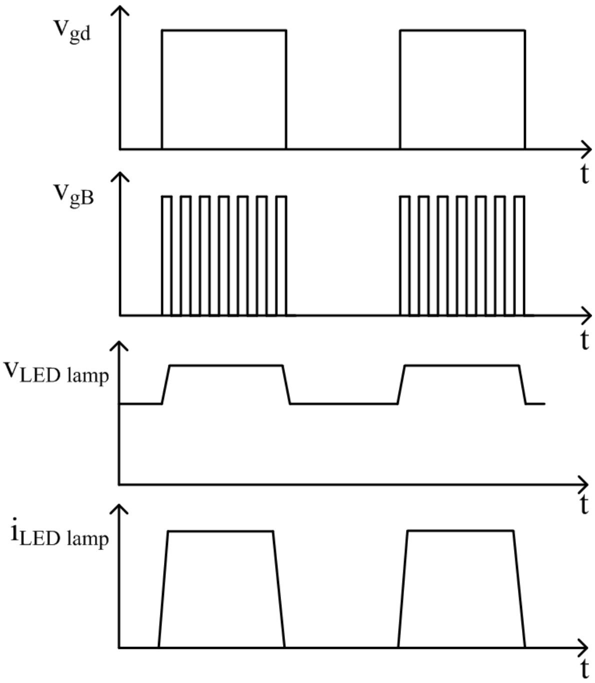

Figure 4: Waveforms under dimming control

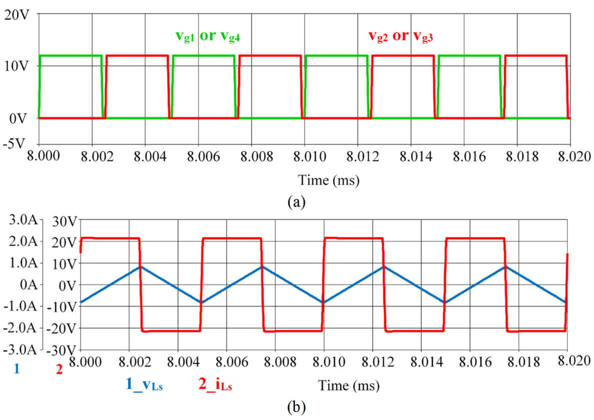

Figure 5: Simulation waveforms (a) Gate voltages of switches in full bridge. (b) Voltage and current in L_s.

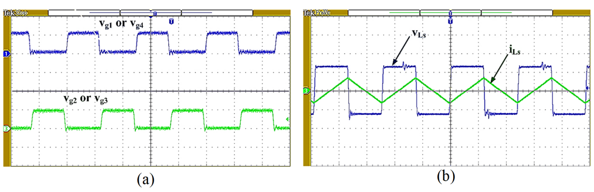

Figure 6: Experimental waveforms (a) Gate voltages of switches in full bridge (v_{g1}, v_{g2}, v_{g3}, v_{g4}: 14 V/div; time: 2 µs/div). (b) Voltage and current in L_s (v_{Ls}: 14 V/div; i_{Ls}: 1 A/div; time: 2 µs/div).

Table 1: Parameters of the proposed LED driver

DC Input voltage, Vin	18 V
DC voltage source, V1, V2	24 V
Number of LEDs	80
LED operating current	550 mA
Switching frequency, fs	200 kHz
Duty ratio of switches in full bridge	0.5
L1, L2, L3, and L4	205 µH
Ls	33 µH
PWM dimming frequency	100 Hz
Duty ratio of dimming switch Sd	0 to 1
Capacitor, C	330 µF/25 V
Frequency of buck-boost converter	100 kHz
Switching devices used	MOSFET IRF640N

6 Simulation and Experimental Results

The proposed LED driver is simulated using OrCAD PSpice software. The parameters used in the simulation are given in Table 1. For experimental validation, a 145 W prototype was developed. Fig. 5 and 6 show the simulation and experimental results of gate voltages of switches in full bridge, voltage and current in L_s respectively. It is observed that the switches in full bridge are operated with fixed duty at 200 kHz. The voltage and current in L_s are in good agreement. Fig. 7 and 8 show the simulation and experimental results of voltage and current in four LED lamps at full illumination level. It is observed that LED lamp current and voltage waveforms have small ripples and they are in good agreement. To show the ZVS feature in switches in full bridge, experimental voltage and current waveforms of switches in one leg are shown Fig. 9 (a) and (b). It is clearly noted that turn ON and turn OFF transitions are completed at zero voltage. Also, switches conduct only i_{Ls} and ripple current in the LED lamp. Hence, conduction losses are independent of lamp currents and they are minimized significantly. Therefore the overall efficiency of the proposed LED driver is high and found to be 95.16% at full illumination level.

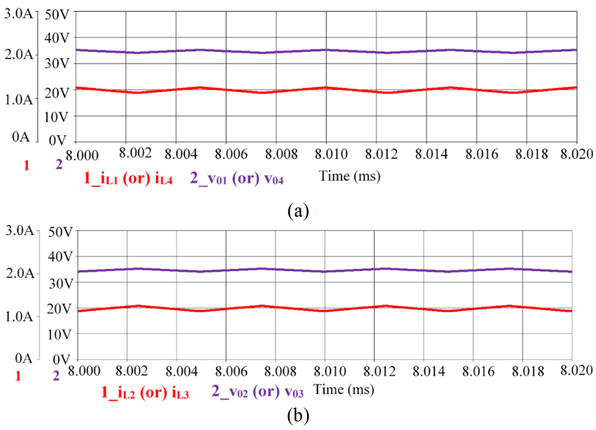

Figure 7: Simulation waveforms (a) Voltage and current waveforms at full illumination in LED lamp-1 and lamp-4. (b) Voltage and current waveforms at full illumination in LED lamp-2 and lamp-3.

Fig. 10 and 11 show gate control voltage of S_d, S_B and all lamp currents at 60% and 80% dimming respectively.It is observed that lamp currents are at their nominal values when the dimming switch is ON and they become zero when dimming switch is OFF. Under 60% and 80% dimming control, the efficiencies of proposed LED driver are found to be 93.8% and 94.47% respectively.

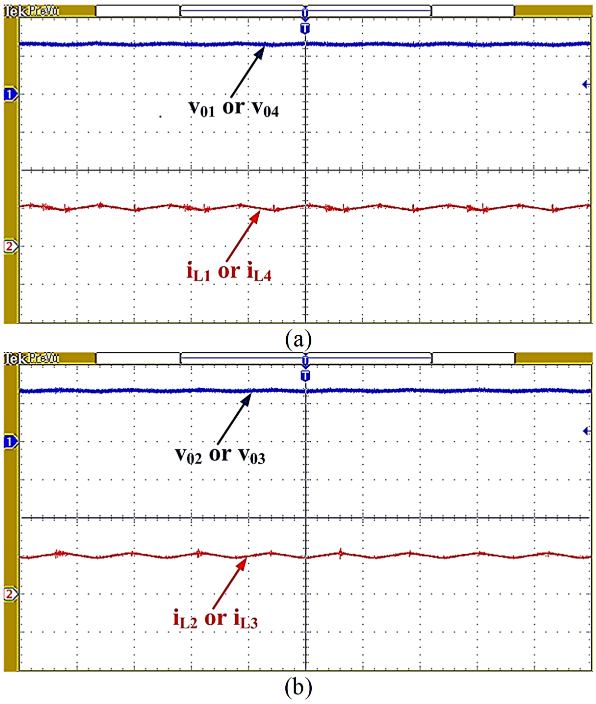

Figure 8: Experimental waveforms (a) Voltage and current waveforms at full illumination in LED lamp-1 and lamp-4. (b) Voltage and current waveforms at full illumination in LED lamp-2 and lamp-3 (v_{01}, v_{02}, v_{03}, v_{04}: 25 V/div; i_{L1}, i_{L2}, i_{L3}, i_{L4}: 1 A/div; time: 8 µs/div).

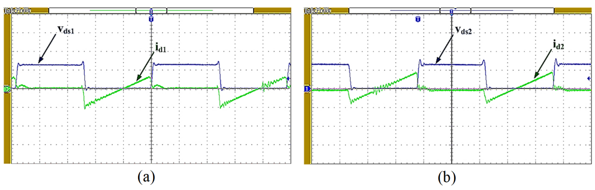

Figure 9: Experimental switching waveforms (a) Voltage and current in Switch S_1(b) Voltage and current in Switch S_2 (v_{ds1}, v_{ds2},: 14 V/div; i_{d1}, i_{d2}: 1 A/div; time: 1 µs/div).

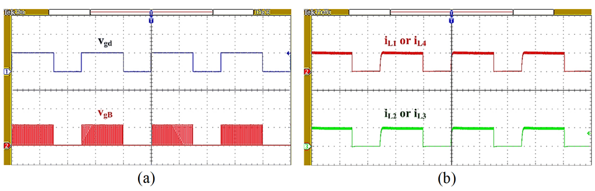

Figure 10: Dimming waveforms at 60% of lamp power (a) Gate control voltages of S_d and S_B(b) Current waveforms of all four lamps (i_{L1}, i_{L2}, i_{L3}, i_{L4}: 1 A/div; time: 4 ms/div)

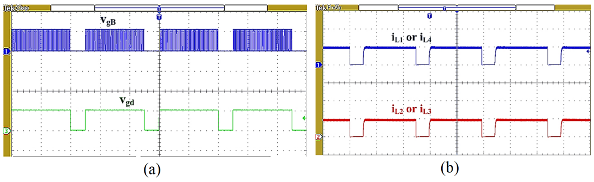

Figure 11: Dimming waveforms at 80% of lamp power (a) Gate control voltages of S_d and S_B(b) Current waveforms of all four lamps (i_{L1}, i_{L2}, i_{L3}, i_{L4}: 1 A/div; time: 4 ms/div)

7 Conclusions

This paper proposes an input controlled full bridge LED driver circuit for driving multiple LED lamps. The losses in full bridge are minimized due to lower processing power. In addition, the current stress of switches in full bridge is reduced. Thus, high on-state resistance switches can be employed. Also, zero-voltage switching feature in the proposed driver leads to high efficiency. PWM dimming control is implemented for all LED lamps. LED lamp currents against input voltage variation can be regulated by using a buck-boost converter at the input stage. This topology may be suitable for PV or battery operated systems.

8 Acknowledgment

The authors gratefully acknowledge the financial support of Technical Education Quality Improvement Programme Phase - III (TEQIP-III), Jawaharlal Nehru Technological University (JNTU), Hyderabad.

References

1.Reddy, U.R., and Narasimharaju, B.L. (2017) Single-stage electrolytic capacitor less non-inverting buck-boost PFC based AC-DC ripple free LED driver,. *IET Power Electronics,*, **pp.38-46, 10 (1)**.

2.Iturriaga-Medina, S., Martinez-Rodriguez, P.R., Juarez-Balderas, M., Sosa, J.M., and Limones, C.A. (2015) A buck converter controller design in an electronic drive for LED lighting applications,. *IEEE International Autumn Meeting on Power Electronics and Computing (ROPEC), pp.1-5*.

3.Agrawal, A., Jana, K.C., and Shrivastava, A. (2015) A Review of Different DC/DC Converters for Power Quality Improvement in LED Lighting Load,. *2015 International Conference on Energy Economics and Environment (ICEEE), pp.1-6*.

4.Bender, V.C., Marchesan, T.B., and Alonso, J.M. (2015) Solid-State Lighting A Concise Review of the State of the Art on LED and OLED Modeling,. *IEEE industrial electronics magazine,*, **pp.6-16, 9(2)**.

5.Li, S., Tan, S.-C., Lee, C.K., Waffenschmidt, E., Hui, S.Y., and Tse, C.K. (2016) A survey classification, and critical review of light-emitting diode drivers. *IEEE Transactions on Power Electronics,*, **pp.1503-1516, 31 (2)**.

6.Wang, Y., Alonso, J.M., and Ruan, X. (2017) A Review of LED Drivers and Related Technologies,. *IEEE Transactions on Industrial Electronics,*, **pp.5754-5765, 64 (7)**.

7.Kim, H.-C., Choi, M.C., Kim, S., and Jeong, D.-K. (2017) An AC-DC LED Driver With a Two-Parallel Inverted Buck Topology for Reducing the Light Flicker in Lighting Applications to Low-Risk Levels,. *IEEE Transactions on Power Electronics,*, **pp.3879-3891, 32 (5)**.

8.Qiu, Y., Wang, L., Wang, H., Liu, Y.-F., and Sen, P.C. (2015) Bipolar Ripple Cancellation Method to Achieve Single-Stage Electrolytic-Capacitor-Less High-Power LED Driver,. *IEEE Journal of Emerging and Selected Topics in Power Electronics,*, **pp.698-713, 3 (3)**.

9.Wang, Y., Huang, J., Wang, W., and Xu, D. (2016) A Single-Stage Single-Switch LED Driver Based on Class-E Converter,. *IEEE Transactions on Industry Applications,*, **pp.2618-2626, 52 (3)**.

10.Moon, S.C., Koo, G.-B., and Moon, G.-W. (2015) Dimming-Feedback Control Method for TRIAC Dimmable LED Drivers,. *IEEE Transactions on Industrial Electronics,*, **pp.960-965, 62 (2)**.

11.Reddy, U.R., Narasimharaju, B.L., and Md, A. (2018) Voltage mode control dcm hsd-cib pfc converter for hb-led lighting applications,. *Journal of Power Technologies,*, **98 (4), pp.305–313,**.

12.Garcia, J., Calleja, A.J., Corominas, E.L., Vaquero, D.G., and Campa, L. (2011) Interleaved Buck Converter for Fast PWM Dimming of High-Brightness LEDs,. *IEEE Transactions on Power Electronics*, **pp. 2627-2636, 26 (9)**.

13.Yu, W., Lai, J.-S., Ma, H., and Zheng, C. (2011) High-Efficiency DC-DC Converter With Twin Bus for Dimmable LED Lighting,. *IEEE Transactions on Power Electronics,*, **pp.2095-2100, 26 (8)**.

14.Santos Filho, E.E. dos, Miranda, P.H.A., Sa, E.M., and Antunes, F.L.M. (2014) A LED Driver With Switched Capacitor,. *IEEE Transactions on Industry Applications*, **pp.3046-3054, 50 (5)**.

15.Pollock, A., Pollock, H., and Pollock, C. (2015) High Efficiency LED Power Supply,. *IEEE Journal of Emerging and Selected Topics in Power Electronics*, **pp.617-623, 3 (3)**.

16.Hwu, K.I., Jiang, W.Z., and Chen, W.H. (2018) Automatic current-sharing extendable two-channel LED driver with non-pulsating input current and zero dc flux,. *International Journal of Circuit Theory and Applications*, **1462-1484, 46 (8)**.

17.Udumula, R.R., Hanumandla, D., and Bellapu, V. (2020) Closed Loop Voltage Mode Controlled High Step-Down/Step-Up Positive Output Buck–Boost Converter,. *Journal of Power Technologies*, **100 (3), 255–262**.

18.Reddy, U.R., and Koppolu, K.K. (2019) Design of Dimmable Light Emitting Diode Driver for Low Power Applications,. *Journal of Power Technologies,*, **99 (3), 204–209**.

19.Castro, I., Lamar, D.G., Lopez, S., Martin, K., Arias, M., and Sebastian, J. (2018) A Family of High Frequency AC-LED Drivers Based on ZCS-QRCs. *IEEE Transactions On Power Electronics,*, **33 (10), 8728-8740.**.

20.Ramakrishnareddy, C.K., Porpandiselvi, S., and Vishwanathan, N. (2019) A three-leg resonant converter for two output LED lighting application with independent control,. *International Journal of Circuit Theory and Applications,*, **47 (7), 1173–1187.**.

21.Alonso, J.M., Perdigao, M.S., Costa, M.A.D., Martinez, ilberto, and Osorio, R. (2017) Analysis and Experiments on a Single-Inductor Half-Bridge LED Driver With Magnetic Control,. *IEEE Transactions On Power Electronics,*, **32 (12), 9179-9190.**.

22.Chen, X., Huang, D., Li, Q., and Lee, F.C. (2015) Multichannel LED Driver With CLL Resonant Converter,. *IEEE Journal Of Emerging And Selected Topics In Power Electronics,*, **3 (3), 589-598.**.

23.Veeramallu, V.K.S., S., P., and L., N.B. (2019) A buck-boost integrated high gain non-isolated half-bridge series resonant converter for solar PV/battery fed multiple load LED lighting applications. *International Journal of Circuit Theory and Applications*, **pp.266-285, 48 (2)**.

24.Reddy, U.R., and Narasimharaju, B.L. (2017) A Cost-Effective Zero-Voltage Switching Dual-Output LED Driver,. *IEEE Transactions on Power Electronics*, **pp.7941-7953, 32 (10)**.

25.Ribas, J., Quintana-Barcia, P.J., Cardesin, J., Calleja, A.J., and Corominas, E.L. (2018) LED Series Current Regulator Based on a Modified Class-E Resonant Inverter,. *IEEE Transactions on Industrial Electronics*, **pp.9488-9497, 65 (12)**.

26.Khatua, M., Kumar, A., Yousefzadeh, V., Sepahvand, A., Doshi, M., Maksimovic, D., and Afridi, K.K. (2020) High-Performance Megahertz-Frequency Resonant DC-DC Converter for Automotive LED Driver Applications,. *IEEE Transactions on Power Electronics,*, **pp.10396-10412., 35 (10)**.